sustainability

MDPI

Article

Hydrologically Derived Winter Water Level Targets and Replenishment Requirements for Sustainable Management of a Regulated Plain River Network

Yu Zhang [1,2], Geng Niu [2,*], Guanhang Sui [3], Tianchi Duan [2], Tian Cheng [2] and Yue Xin [4]

[1] College of Water Conservancy and Hydropower Engineering, Hohai University, Nanjing 210024, China; zyu21@hhu.edu.cn
[2] State Key Laboratory of Water Cycle and Water Security, China Institute of Water Resources and Hydropower Research, Beijing 100038, China; duantianchi@edu.iwhr.com (T.D.); chengtian@edu.iwhr.com (T.C.)
[3] Beijing Key Laboratory of Urban Hydrological Cycle and Sponge City Technology, College of Water Sciences, Beijing Normal University, Beijing 100875, China; suiguanhang@mail.bnu.edu.cn
[4] School of Water Conservancy and Hydroelectric Power, Hebei University of Engineering, Handan 056038, China; xyue22569@163.com
* Correspondence: niugeng@iwhr.com

Abstract

Winter water allocation in regulated plain river networks requires an operational link between hydrological low water benchmarks and replenishment decisions. This study focused on the Lixiahe plain river networks; utilizing winter water level records from nine stations during 2006–2021, five hydrological methods were applied to derive candidate water level benchmarks. A one-dimensional MIKE 11 model was applied to simulate total upstream replenishment scenarios of 40–400 m^3/s and to establish station-specific stage–discharge relationships under fixed downstream boundaries and structure operation rules. Within the simulated range, the candidate benchmarks corresponded to scenario-specific replenishment requirements of 153.94–268.49 m^3/s. The framework supports comparison of winter water allocation strategies and identification of controlling stations, but ecological sufficiency requires independent evidence from species, habitat, thermal, dissolved oxygen, and water quality responses.

Keywords: plain river network; hydrological water level benchmark; hydrodynamic simulation; replenishment threshold; sustainable water management

Check for updates

Academic Editor: Agostina Chiavola

Received: 9 July 2026
Revised: 18 August 2026
Accepted: 20 August 2026
Published: 21 August 2026

Copyright: © 2026 by the authors. Licensee MDPI, Basel, Switzerland. This article is an open access article distributed under the terms and conditions of the Creative Commons Attribution (CC BY) license.

1. Introduction

Plain river networks are characterized by low channel gradients, dense river–lake connections, and complex hydraulic controls [1]. In such systems, water levels and flow directions are jointly affected by sluices, pumping stations, polder drainage, external water diversion, and downstream boundary conditions [2,3]. During winter, reduced precipitation and natural inflow weaken hydraulic exchange within the river network, which may lead to insufficient water depth, low flow velocity, reduced connectivity, and degradation of aquatic habitats. Unlike single-channel rivers, plain river networks do not exhibit a simple one-to-one relationship between upstream replenishment discharge, water-level rise, and hydrodynamic response. Winter management therefore involves two distinct questions: which water level benchmarks are defensible from the available evidence [4,5], and what upstream replenishment is required to attain those benchmarks under specified operating conditions [6]?

A variety of methods have been developed for estimating ecological water levels and environmental flows. Among them, hydrological statistical methods are widely used [7,8] because they require relatively limited data, are easy to implement, and produce results that can be readily interpreted for water management. Frequency-based water levels, duration curves, and low water frequency methods [9] can extract characteristic low water conditions from long-term hydrological records and provide a historical reference for minimum water levels targets. However, these methods mainly describe the occurrence probability of historical water levels. They cannot directly reveal the hydraulic response of a complex river network under different replenishment scenarios, nor can they quantify the engineering discharge required to achieve a specific water level target. In heavily regulated plain river networks, water level targets derived solely from historical statistics may therefore be disconnected from actual operational capacity, replenishment pathways, and spatial water level responses [10,11].

Hydrodynamic modeling provides an effective way to bridge ecological water level targets and engineering operation [12,13]. By simulating water level changes at key stations under different upstream replenishment scenarios, a hydrodynamic model can reveal the spatial heterogeneity of replenishment effects and establish quantitative relationships between upstream inflow and station water levels [14,15]. Coupling hydrological-statistical water level candidates with fitted stage–discharge response curves makes it possible to invert the upstream total replenishment discharge required to satisfy different water level targets. In this way, the water management question of "what water level should be maintained" can be transformed into the operational question of "how much water should be supplied".

The Lixiahe region in central-northern Jiangsu Province is a typical plain river network in eastern China [16,17]. The region contains dense rivers, channels, lakes, and polders, and its water level regime is strongly influenced by water replenishment from the Jiangdu and Gaogang hubs as well as by regional sluice and pumping operations. Winter is both a dry season and a sensitive period for ecological water level maintenance, making it a critical period for identifying minimum ecological water level requirements and replenishment thresholds [18]. Studying the Lixiahe region can improve understanding of how external replenishment is transmitted through a regulated plain river network [19,20] and can provide practical reference for winter water replenishment in similar regions [21].

Previous studies of plain river networks have examined river–lake–sluice hydrodynamics, connectivity, water quality responses to diversion, and joint sluice–pump operation. However, fewer studies have compared several winter low water benchmarks across multiple control stations and translated each benchmark into a regional upstream replenishment requirement under a consistent set of operating conditions. The present study addresses this operational linkage, while recognizing that the resulting benchmarks still require ecological validation.

In this study, the Lixiahe plain river network was selected as the study area. Winter water level records from nine control stations during 2006–2021 were used to estimate hydrologically based water level target through multiple hydrological methods, including the guarantee rate method, monthly guarantee rate method, intra-annual distribution method, annual minimum monthly mean method, and 7-day low water frequency method. A one-dimensional MIKE 11 hydrodynamic model was then constructed to simulate water level responses under different upstream total replenishment discharge scenarios. Based on the fitted relationships between water level and input discharge, the upstream replenishment thresholds required to meet hydrologically based water level targets were identified.

2. Materials and Methods

2.1. Study Area

The Lixiahe region is located in central-northern Jiangsu Province and in the lower Huaihe River Basin (Figure 1). It is a typical plain river network area situated between the lower Yangtze River plain and the Huaihe River sea outlet corridor. The study area lies approximately between 119°12′–120°56′ E and 32°12′–34°10′ N, extending from the Grand Canal in the west to the Tongyu River in the east, and from the North Jiangsu Irrigation Canal in the north to the New Tongyang Canal in the south. It covers parts of Yancheng, Taizhou, Yangzhou, Huai'an, and Nantong, with a total area of approximately 13,500 km^2.

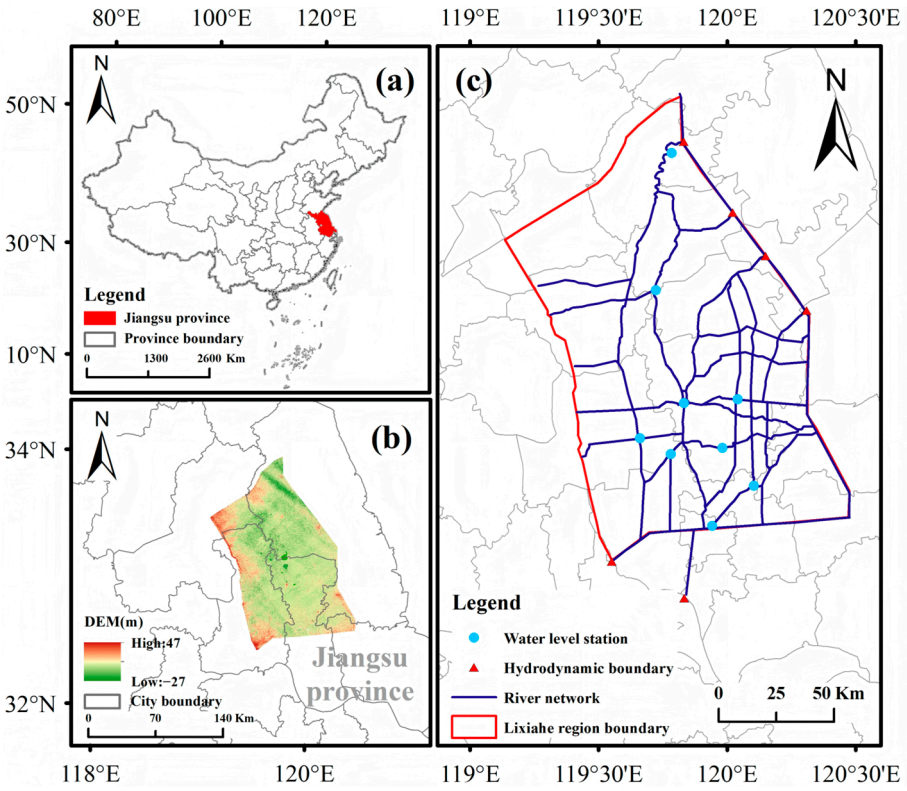


Figure 1. Overview of the study area. (**a**) Location of Jiangsu Province in China; (**b**) location of the Lixiahe Plain in Jiangsu Province; (**c**) water level stations, hydrodynamic boundary and river network in the Lixiahe region.

The study area is geomorphologically characterized by low-lying flat terrain, with the central part showing a distinct basin-like pattern of higher margins and a lower interior. Rivers, ditches, lakes, and shallow lake depressions are interlaced across the region, forming a dense water system with complex flow directions. Natural topographic gradients are small, and river network water levels are jointly affected by precipitation, inflow from external rivers, polder drainage, and water diversion projects. Water exchange is frequent, and the hydrological processes exhibit pronounced artificial regulation. Regional drainage is generally organized from southwest to northeast, while the main water sources are the Jiangdu and Gaogang water control hubs. In the central area, water is mainly discharged into the Yellow Sea through backbone sea outlet channels such as the Sheyang River, Huangsha Port, Xinyang Port, and Doulong Port; during flood seasons, part of the water may also be diverted toward the Yangtze River through engineering facilities such as the Jiangdu Pumping Station. This complex hydraulic system gives the study area the dual characteristics of a natural plain river network and an engineering-controlled river network.

From the perspective of human activities, the Lixiahe region has long supported multiple functions, including agricultural production, urban development, Yangtze River water diversion, water conveyance for the eastern route of the South-to-North Water Diversion Project, and the protection of lake and wetland ecosystems. Since the 1950s, regional water conservancy development has progressed through river dredging, polder management, construction of water diversion and drainage channels, lake restoration, and coordinated water network operation. These efforts have substantially improved flood control, drainage, and water supply capacities and have gradually formed a regional water-network pattern supported by backbone channels and lake nodes. However, rapid urbanization has placed considerable pressure on the regional aquatic ecological condition, and intensified artificial drainage has further aggravated hydraulic imbalance.

2.2. Data Sources and Processing

For the hydrodynamic model, the river channel model requires information on river network topology, cross-sectional geometry, and physical parameters such as bed roughness and bank roughness. The hydrodynamic boundary conditions include inflow discharge into the study area and downstream water levels.

River channel topology was derived from the 1:250,000 National Fundamental Geographic Database, which provides vector map data. The hydrological features include areal water bodies, linear water system features, and point water system features, corresponding respectively to lakes and reservoirs; single-line rivers, ditches, and river structural lines; and springs and wells. The data were obtained from the National Geomatics Information Resource Directory Service System.

Some river cross-section data were obtained from Hydrological Yearbook of the Huaihe River Basin. For data-sparse channels, cross-section water depth surveys were implemented in the field with a portable ultrasonic depth sounder (Model WX-CS50; Shandong Wanxiang Environmental Technology Co., Ltd., Weifang, China). River-bed elevation, channel width, and bank slope ratio were generalized appropriately in combination with local river regulation conditions. Roughness values were initially generalized based on observations of bank materials and bed conditions and were subsequently optimized during hydrodynamic model calibration.

Hydrological data were also obtained from the Hydrological Yearbook of the Huaihe River Basin for 2006–2021. Daily water level and discharge records for the available stations were digitized from the yearbooks. The water level records were used for station-specific hydrological frequency analyses, whereas the Jiangdu and Gaogang discharge records were used to characterize winter external replenishment and to define the hydrodynamic boundary and simulation conditions.

Data preprocessing included unifying the elevation datum, checking missing and anomalous values, removing abrupt changes clearly caused by non-hydrological factors, and ensuring temporal comparability among water level series from different stations. Short missing segments at individual gauges were interpolated using daily hydrograph patterns at neighboring stations, whereas series with prolonged missing periods were excluded from frequency fitting. Zero values in the Jiangdu and Gaogang discharge records were retained when they represented genuine days without external replenishment. These values were not treated as missing observations, removed from the dataset, or replaced with arbitrary small positive values.

2.3. Construction and Parameter Calibration of the River Network Hydrodynamic Model

In this study, the MIKE 11 (version 2014; DHI, Hørsholm, Denmark) HD module was used to construct a one-dimensional hydrodynamic model [12,13] of the river network

in the study area. MIKE 11 is suitable for simulating unsteady flow in river networks, and plain river networks regulated by sluices and pumping stations [14,15]. Its core concept is to generalize natural channels into a one-dimensional topological network [21,22] composed of reaches, cross sections, nodes, and hydraulic structures, and to solve the temporal variation of water levels and discharges within the river network under prescribed boundary conditions, initial conditions, channel roughness, and related parameters.

Considering the dense river network, low-lying terrain, and strong human regulation in the Lixiahe region, the model was constructed with backbone conveyance channels and major connecting tributaries as the main objects. Control structures such as sluices and pumping stations were embedded as internal structures in the river network system to represent hydrodynamic processes including channel conveyance and discharge to the sea.

2.3.1. Principles of the Hydrodynamic Model

One-dimensional unsteady channel flow is governed by the Saint–Venant equations [13,14]. This equation system consists of the continuity equation and the momentum equation, representing conservation of mass and conservation of momentum, respectively. Its commonly used form is as follows:

$$\frac{\partial A}{\partial t} + \frac{\partial Q}{\partial x} = q, \tag{1}$$

$$\frac{\partial Q}{\partial t} + \frac{\partial}{\partial x}\left(\alpha \frac{Q^2}{A}\right) + gA\frac{\partial H}{\partial x} + gAS_f = 0, \tag{2}$$

where x is the distance along the channel; t is time; A is the flow cross-sectional area; Q is the discharge through the cross section; q is the lateral inflow or outflow per unit channel length; H is the water level; g is gravitational acceleration; α is the momentum correction coefficient; and S_f is the friction slope. The friction term is commonly expressed using the Manning formula:

$$S_f = \frac{n^2 Q|Q|}{A^2 R^{4/3}}, \tag{3}$$

where n is the Manning roughness coefficient; $R = A/P_w$ is the hydraulic radius, and P_w is the wetted perimeter.

The above equations are based on assumptions such as cross-sectionally averaged velocity and hydrostatic pressure distribution. For plain river networks, these equations can describe gradually varied unsteady flow, water level propagation induced by sluice and pump regulation, and flow redistribution at network nodes.

2.3.2. Model Development Procedure

The model development procedure mainly included river network generalization, cross-section data processing, boundary condition setting, and hydraulic structure parameterization. First, based on water system data, channel centerlines, measured cross sections, and the distribution of hydraulic works in the study area, the calculated reaches and their topological connections [21,22] were determined and a Network file was established (Figure 2). A Cross-section file was then created using measured cross-section data and generalized cross-sectional forms. In the Boundary file, upstream inflow discharge and downstream water level boundary conditions [23] were specified based on hydrological data. For sluices and pumping stations, gate width, sill elevation, discharge coefficients, pump characteristic curves, and operating rules were entered through the Structure file. Finally, the Simulation file was configured to call the relevant files and define the simulation period, time step, spatial step, initial water levels, and output settings, thereby forming a complete hydrodynamic simulation scheme.

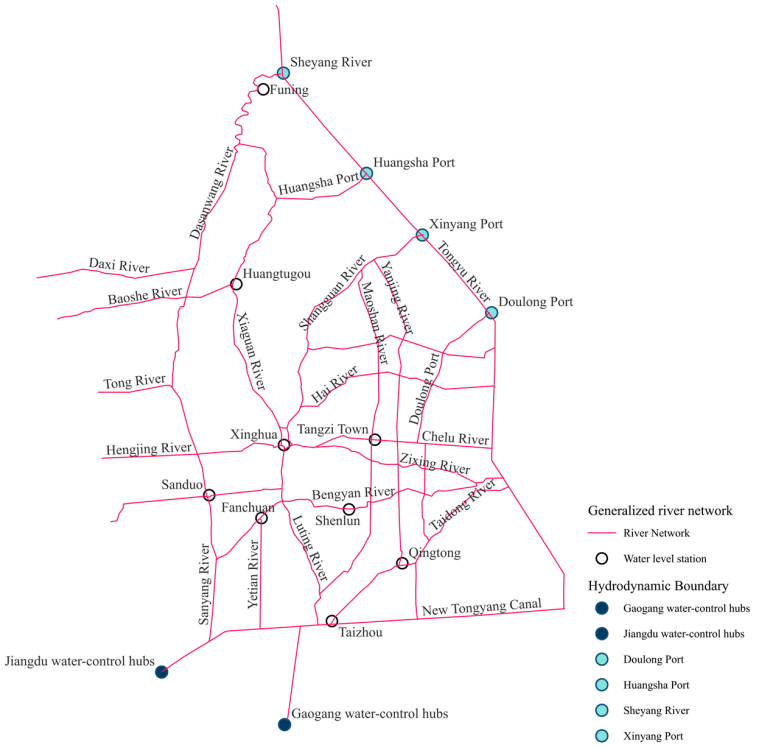


Figure 2. Schematic diagram of the generalized river network.

For plain river networks strongly affected by sluice and pump operation, large differences between initial water levels and boundary water levels can easily produce numerical oscillations during the initial stage of computation. Therefore, a warm-up period was set before the formal simulations so that water levels, discharges, and hydraulic structure operating states in the river network could gradually become coordinated. Boundary conditions were specified using synchronized observed data with a consistent time reference.

2.3.3. Parameter Calibration Procedure

Parameter calibration focused primarily on channel roughness while also considering sensitive factors such as local resistance coefficients, gate discharge coefficients, pump operating parameters, and initial water levels. The Manning roughness coefficient reflects the combined effects of bed material, bank vegetation, and cross-sectional form, and is the most important parameter to be determined in a one-dimensional river network model [14,15].

During the calibration period, initial river roughness values (Table 1) were assigned according to channel type based on the approximate ranges reported in the literature [24]. The roughness coefficient of each river reach was then calibrated individually by comparing the simulated water levels with the observations at the corresponding stations. The coefficients were adjusted reach by reach until the simulated water-level processes agreed satisfactorily with the observations in terms of water level fluctuations, peak timing, and peak water levels.

Table 1. Literature-based initial value of river roughness.

Channel Characteristics	Initial Manning Value
Basin-scale trunk watercourse	0.022
Regional major watercourse	0.024
Major cross-county watercourse	0.028
Key county-scaled watercourse	0.028

2.4. Design of Winter Replenishment Discharge Scenarios and Construction of River Network Stage–Flow Response Relationships

To identify the regulatory effect of external water replenishment on river network water levels in the Lixiahe region during winter, this study used the Jiangdu and Gaogang water control hubs as the main upstream replenishment boundaries, designed winter replenishment discharge scenarios, and established response relationships between water levels at key regional stations and upstream input discharge based on the calibrated river network hydrodynamic model [12,21].

Because winter in the study area corresponds to the dry season and a sensitive period for water level maintenance, the scenario design used December, January, and February as the statistical period. Concurrent discharges from the Jiangdu and Gaogang hubs were treated as the principal components of external input discharge. At any time t, the total external input discharge into the region can be expressed as

$$Q_{ext}(t) = Q_{JD}(t) + Q_{GG}(t), \tag{4}$$

where $Q_{ext}(t)$ is the total external input discharge entering the Lixiahe region, in m^3/s; $Q_{JD}(t)$ and $Q_{GG}(t)$ are the input discharges from the Jiangdu and Gaogang water control hubs, in m^3/s.

Zero discharge observations represented genuine days without external replenishment. They were retained in the analysis and were not treated as missing values or replaced with arbitrary small positive values. For each discharge series, the zero discharge probability was calculated as $p_0 = N_0/N$, where N_0 is the number of zero discharge observations and N is the total number of valid observations. Following the conditional-probability approach used in established streamflow frequency analyses [25], zero discharges were represented as a discrete probability mass, whereas the P-III distribution was fitted only to positive discharges.

Let $F_+(q)$ denote the conditional cumulative distribution fitted to positive discharges. The overall mixed distribution was expressed as

$$F(q) = \begin{cases} 0, & q < 0, \\ p_0, & q = 0, \\ p_0 + (1 - p_0)F_+(q), & q > 0, \end{cases} \tag{5}$$

where $F(q)$ is the overall cumulative probability of winter daily input discharge. Positive observations were ranked separately to determine their conditional empirical frequencies. Repeated zero observations were represented collectively by p_0 rather than being assigned different plotting positions.

In this study, the discharge guarantee rate was defined as the overall exceedance probability. For $q > 0$, the overall and conditional exceedance probabilities were related by

$$P_e(q) = (1 - p_0)P_{e,+}(q), \tag{6}$$

where $P_{e,+}(q) = P(Q \geq q \mid Q > 0)$. When a target guarantee rate exceeded the observed positive discharge probability $1 - p_0$, no positive discharge quantile was available, and the corresponding discharge was set to zero. Negative extrapolated discharges were not retained or used to determine management thresholds.

The conditional exceedance probabilities obtained from the positive inflow sample were multiplied by the observed positive inflow probability, $1 - p_0$, to obtain the corresponding overall exceedance probabilities. The resulting mixed probability distribution, including the discrete zero inflow component (Figure 3).

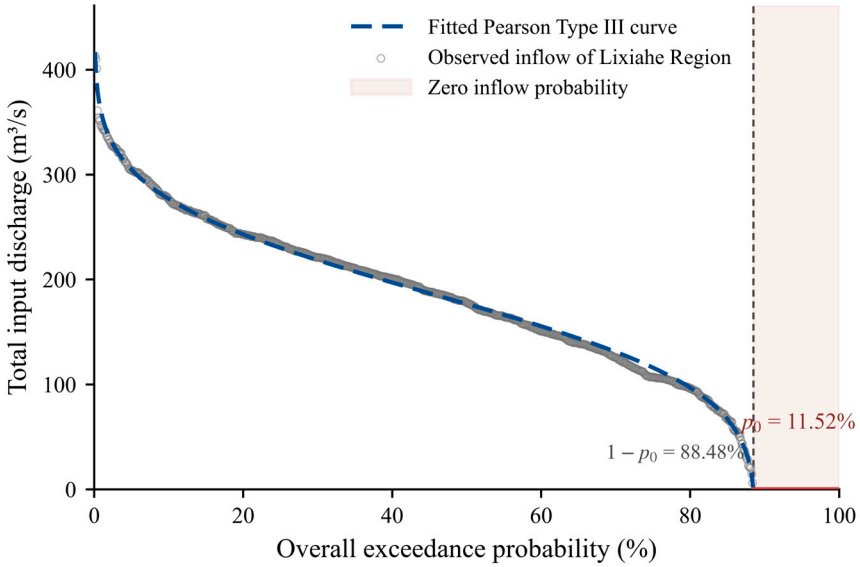


Figure 3. Frequency fitting curves for upstream winter daily inflow.

In scenario design, this study considered both the representativeness of historical hydrological conditions and the need to identify model response characteristics. On one hand, based on the winter external input discharge guarantee rate table for the Jiangdu and Gaogang water control hubs, input discharges corresponding to several typical guarantee rates were selected as hydrologically representative scenarios to characterize the winter replenishment background. On the other hand, equal gradient replenishment simulation scenarios were established to construct continuous stage–flow response relationships. Considering existing hub water diversion operating conditions and model stability requirements, 10 discharge levels of 20, 40, 60, 80, 100, 120, 140, 160, 180, and 200 m^3/s were set separately for the Jiangdu and Gaogang hubs. When the two hubs increased synchronously, the corresponding total external input discharge for the region ranged from 40 to 400 m^3/s.

All replenishment scenarios were run under consistent channel parameters and downstream boundary conditions, using multi-year average winter water levels, to ensure comparability among scenarios. To highlight the marginal effect of upstream replenishment discharge on regional water levels, the winter simulations kept downstream water level boundaries, initial water level conditions, and major engineering operating rules consistent. Sluices were maintained under conventional opening or fixed control states, while pumping stations were treated as closed or fixed discharge boundaries. These simplifications were intended to isolate the interference of complex sluice pump operation on the stage–response relationship, so that the established Q-H relationship primarily reflected the influence of variations in external replenishment discharge. Future multi-objective operation studies may further introduce scenarios involving gate openings, pumping station discharges, and combinations of zonal operations.

These assumptions were adopted to isolate the response to total upstream replenishment. Consequently, the fitted relationships should be interpreted as conditional response functions rather than transferable rating curves.

After model runs were completed, simulated water level processes were extracted for key water level stations such as Xinghua, Fanchuan, and Sanduo. To reduce the influence of initial conditions and short-term fluctuations on the response relationships, the mean daily water level over the winter simulation period was used as the representative water level for each scenario.

Because plain river networks are influenced by network storage regulation, cross-sectional conveyance capacity, downstream water level control, and local backwater effects,

the response of water level to upstream replenishment discharge may not be strictly linear. To balance functional interpretability with the ability to represent changes in marginal response, this study used a quadratic polynomial as the unified fitting form for the Q-H response relationships at key stations:

$$H_i = a_i Q^2 + b_i Q + c_i + \varepsilon_i, \tag{7}$$

where a_i, b_i, and c_i are the quadratic coefficient, linear coefficient, and constant term of the response curve for station i, respectively; Q is the external input discharge, in m^3/s; and H_i is the representative water level at station i under the corresponding scenario, in m.

2.5. Derivation of Hydrologically Based Candidate Water Level Benchmarks

Hydrological frequency analysis uses the statistical distribution characteristics of historical water level series to identify representative water levels under different guarantee rates, thereby providing hydrological context and an initial reference for determining dry season water levels. For a plain river network such as the Lixiahe region, which is jointly affected by sluices and pumps, water diversion and drainage projects, and external replenishment, historical water level processes reflect both natural regional hydrological conditions and the combined effects of engineering regulation and water resource use.

Hydrological frequency analysis characterizes the probability and persistence of historical winter water levels. In this study, the resulting values are termed hydrologically derived candidate water level benchmarks. They provide a transparent basis for comparing low water conditions and management scenarios, but they are not interpreted as biologically sufficient ecological thresholds. Biological validation would require explicit information on local species, habitat, substrate, temperature, dissolved oxygen, and water quality.

This study used December, January, and February as the winter analysis period and extracted daily water level series for each water level station in the study area. To maintain the continuity of winter processes, winter samples were processed by hydrological year; that is, December of a given year and January–February of the following year together formed one complete winter. For the water level station i, the water level guarantee rate means the probability that the water level is not lower than a specified control water level, namely:

$$P(H_i \geq H_{i,p}) = p, \tag{8}$$

where p stands for the dimensionless exceedance probability satisfying $0 < p < 1$, and $H_{i,p}$ denotes the site-specific water level quantile that is met or surpassed at probability p.

A higher guarantee rate generally corresponds to a lower water level, meaning that the water level can be reached with a higher probability during historical winter periods. High guarantee rate water levels are closer to the low water control line of the historical water level duration curve and are therefore suitable as hydrological references for minimum water level targets, although their ecological rationality still requires verification.

Empirical frequency calculations were first performed for the winter water level samples at each station. The water level series was sorted in descending order, and the water level was denoted as $H_{i,m}$. Its empirical guarantee rate can then be estimated as follows:

$$P_m = m/(n+1) \times 100\%, \tag{9}$$

where P_m is the empirical guarantee rate corresponding to the water level sample; m is the rank order; and n is the total number of samples.

The empirical frequency curve can intuitively reflect the duration distribution of winter water levels, but it is strongly affected by sample length, extreme values, and discrete fluctuations. To obtain continuous, smooth, and easily interpolated guarantee rate

water levels, this study further fitted Pearson type III distributions to the winter water level series.

The Pearson Type III (P-III) distribution was selected a priori rather than through an exhaustive comparison of candidate distributions. This choice was based on its three-parameter structure, which can represent the skewness commonly observed in hydrological series, and on its established use in conventional at-site hydrological frequency analysis in China [26]. In this study, P-III was applied consistently across stations to provide comparable frequency-based hydrological quantiles. Its site-specific adequacy was evaluated against the empirical frequency points using R^2, as reported in Section 3.3. Nevertheless, the resulting quantiles are conditional on the selected distribution and the 2006–2021 observation period; therefore, the use of P-III in this study should not be interpreted as evidence that it is universally superior to other probability distributions. Its probability density function can be written as

$$f(x) = \frac{\beta^{\alpha}}{\Gamma(\alpha)}(x - a_0)^{\alpha-1}e^{-\beta(x-a_0)},\ x > a_0, \tag{10}$$

where α and β are the shape and scale parameters, respectively; a_0 is the location parameter; and $\Gamma(\alpha)$ is the Gamma function.

In practical hydrological frequency calculations, the distributional form is characterized by the sample mean, coefficient of variation, and coefficient of skewness. For the winter water level series at station i, the sample mean, coefficient of variation, and coefficient of skewness are defined as follows:

$$\overline{x} = \frac{1}{n}\sum_{i=1}^{n} x_i, \tag{11}$$

$$C_v = \frac{S}{\overline{x}}, \tag{12}$$

$$C_s = \frac{n\sum_{i=1}^{n}(x_i - \overline{x})^3}{(n-1)(n-2)S^3}, \tag{13}$$

where n is the sample size; x_i is the ith sample value; $\overline{x}$ is the sample mean; S is the sample standard deviation; Cv is the coefficient of variation; and Cs is the coefficient of skewness.

According to the Pearson type III frequency curve, the theoretical water level under different guarantee rates is

$$H_p = \overline{H}(1 + C_v\Phi_p), \tag{14}$$

where H_p is the theoretical water level corresponding to the guarantee rate; $\overline{H}$ is the multi-year mean water level; C_v is the coefficient of variation; and Φ_p is the frequency factor of the Pearson type III curve, which can be obtained from Pearson type III frequency curve tables or through numerical calculation.

This study adopted water level determination methods based on the statistical distribution of water levels [26]. To avoid bias caused by reliance on a single threshold method, the guarantee rate method, monthly guarantee rate method [27,28], intra-annual distribution method, annual minimum monthly mean method [29], and 7-day low water frequency method [30,31] were applied comprehensively, and their results were compared.

2.5.1. Guarantee Rate Method

The guarantee rate method uses the water level corresponding to a specified guarantee rate as the water level threshold [4,5]. Its basic premise is that water levels with relatively high persistence probability in a long-term series [6,7] can represent relatively stable low water conditions, which may serve as a statistical benchmark for ecological water level assessment.

The 75%, 90%, and 95% guarantee rates were selected to represent three hydrological-management scenarios rather than biologically determined ecological thresholds. Because the guarantee rate is defined as the probability that the water level is not lower than a specified value, a higher guarantee rate generally corresponds to a lower and more historically attainable water level benchmark. The P75 water level represents a moderately dry but relatively common condition and was included as a higher candidate benchmark associated with a greater replenishment requirement. P90 represents a lower water condition and was adopted as the central comparison level because it provides a practical compromise among low water representativeness, historical attainability, and statistical robustness. P95 was included as a lower-bound, high-attainability scenario under more severe dry conditions and as a means of examining sensitivity to the lower tail of the water level distribution. Together, the three levels provide a graded basis for comparing water level targets and replenishment requirements under different water availability conditions. They should not be interpreted as species-specific or biologically validated ecological thresholds.

Together, these three levels form a guarantee rate gradient from a common moderately dry state to a stricter low water constraint.

2.5.2. Monthly Guarantee Rate Method

The monthly guarantee rate method [27,28] emphasizes the non-uniformity of water level processes within the winter season. This method first constructs monthly empirical frequency curves for December, January, and February separately, and then calculates the water level corresponding to the specified guarantee rate for each month. The monthly guarantee rate water level can be expressed as

$$E_{m,P} = H_{m,P}, m \in \{12,\ 1,\ 2\}. \tag{15}$$

For comprehensive comparison, this study used the mean of the $P = 90\%$ guarantee rate water levels for the three winter months. This indicator retains information on monthly-scale differences while forming a single statistic suitable for comparison among stations.

The monthly guarantee rate analysis was based on winter daily water level records covering 2006–2021. The same analysis period and data processing procedure were applied to all nine stations to maintain comparability among stations. Accordingly, the resulting monthly guarantee levels were used as period-specific hydrological benchmarks for cross-station comparison and operational scenario assessment.

2.5.3. Intra-Annual Distribution Method

The intra-annual distribution method is used to convert the overall winter water level benchmark into a monthly water level process. This method takes the overall winter $p = 90\%$ guarantee rate water level as the baseline and superimposes the anomaly of the multi-year monthly mean water level relative to the winter mean water level:

$$E_m^{dist} = H_{90} + \left(\overline{H_m} - \overline{H_w}\right),\ m \in \{12,\ 1,\ 2\}, \tag{16}$$

where E_m^{dist} is the distributed water level for month m; $\overline{H_m}$ is the multi-year mean water level for month m, and $\overline{H_w}$ is the winter mean water level.

If the mean water level in a given month is higher than the winter mean, the water level for that month is correspondingly increased; otherwise, it is reduced. This method is superior to a single guarantee rate threshold in preserving intra-seasonal water level rhythms.

2.5.4. Annual Minimum Monthly Mean Method

The annual minimum monthly mean method starts from low water processes in individual winters and reduces the influence of single-day extreme fluctuations on water-level estimation. For each complete winter year, monthly mean water levels are first calculated for December, January, and February, and the minimum of these values is then taken as the representative low water level for that winter year.

2.5.5. Seven-Day Low Water Frequency Method

The 7-day low water frequency method [26,30] is used to characterize continuous low water processes. Compared with the single-day minimum water level, the 7-day moving average reduces the influence of short-term random fluctuations and is more suitable for representing low water stress with sustained effects on aquatic ecosystems. For a complete winter, the 7-day moving average water level is defined as

$$\tilde{H}^{(7)}_{Y,t} = \frac{1}{7}\sum_{j=0}^{6} H_{Y,t-j}. \tag{17}$$

The minimum 7-day average water level for that winter is

$$L^{(7)}_{Y} = \min_{t} \tilde{H}^{(7)}_{Y,t}. \tag{18}$$

Empirical frequency analysis of the $L^{(7)}_{Y}$ series yields the water level based on 7-day low water frequency:

$$E_{7d,P} = Q_P\left(L^{(7)}_{Y}\right). \tag{19}$$

This study used $P = 90\%$ as the representative guarantee rate for this method. This indicator is relatively conservative and is suitable for characterizing water level constraints under continuous low water conditions.

2.6. Upstream Replenishment Required to Meet Hydrological Water Level Benchmarks

After determining the hydrological water level targets and the regional river network stage–flow response relationships, this study further identified upstream replenishment discharge thresholds required to meet winter hydrological water level demands. The water level requirements proposed from hydrological considerations were converted into upstream boundary discharge conditions, thereby providing a quantitative basis for winter operation of external replenishment projects such as the Jiangdu and Gaogang water control hubs.

The determination of replenishment discharge or water level thresholds generally needs to consider hydrological processes, habitat requirements, and engineering feasibility. Therefore, it should not rely solely on a single historical statistical value but should be integrated with hydrodynamic responses of the river network.

In the preceding analysis, different winter replenishment scenarios were established using the MIKE river network hydrodynamic model, and response relationships between water levels at control stations and upstream input discharge were fitted. These response relationships were described by quadratic polynomials. The function characterizes the influence of replenishment discharge changes on regional river network water levels within the studied discharge range, and its applicability should be limited to the model calibration conditions and replenishment scenario settings.

At the single-station scale, the replenishment discharge threshold required to meet a hydrological water level target is defined as the minimum replenishment discharge at which the simulated water level reaches or exceeds the water level target:

$$Q_i min = min\{Q | f_i(Q) \geq H_i,\ \ Q_{min} \leq Q \leq Q_{max}\}, \tag{20}$$

where Q_i is the replenishment discharge threshold for station i; Q_{min} and Q_{max} are the minimum and maximum replenishment discharges set in the scenario simulations, respectively.

If the stage–flow response relationship is approximately monotonically increasing within the study range, Q_i can be obtained by inverting the response function. For a quadratic response function, the root that falls within the scenario discharge range and has practical hydrological meaning is selected as the replenishment threshold for the station. If the water level at Q_{min} already satisfies the hydrological water level target, the station meets the requirement under the existing low flow condition. If the water level at Q_{max} remains below the hydrological water level benchmark, the existing replenishment scenarios are insufficient, and the need for engineering operation adjustment or ecological target revision should be discussed in the results.

Because water level responses in the Lixiahe river network show clear spatial differences, the replenishment discharge thresholds required by different stations may not be consistent. Therefore, at the regional scale, single-station thresholds and an all-area satisfaction threshold can be identified separately. When all control stations are included in the evaluation, the regional all-area satisfaction threshold can be expressed as

$$Q_A = max(Q_i), i = 1, 2, \ldots, n. \tag{21}$$

This treatment means that regional replenishment discharge must at least reach the maximum threshold among the control stations to ensure that water level targets are met within the corresponding area. If the research objective focuses on key reaches or ecologically sensitive areas, representative stations may be selected to calculate zonal thresholds, thereby avoiding excessive control of overall replenishment demand by the most unfavorable station across the whole region.

During threshold determination, candidate replenishment discharges should also be checked for engineering feasibility and hydrodynamic rationality. On one hand, the replenishment discharge should not exceed the winter water supply capacity and allowable operating range of the Jiangdu and Gaogang water control hubs. On the other hand, after replenishment, water levels at all control stations should not exceed regional safety control levels, and flow velocities in key reaches should remain within ecologically suitable ranges as far as possible. Accordingly, the final upstream replenishment discharge threshold can be understood as the minimum feasible discharge jointly constrained by water level targets, river network hydrodynamic responses, and engineering operation boundaries. The specific threshold results, differences among control stations, and corresponding replenishment scenarios are further analyzed in the Section 3.

3. Results

3.1. Calibration Results of the Hydrodynamic Model

The hydrodynamic model calibration results indicate that the model achieved acceptable accuracy in simulating low-amplitude winter water level variations and can support scenario comparison and response trend identification. Following the reach-by-reach iterative calibration, the final Manning coefficients ranged from 0.020 to 0.035. These values represent effective roughness parameters under the modeled winter conditions rather than direct measurements of temporally varying physical roughness. Across the nine water level

stations (Table 2), the root mean square error (RMSE) ranged from 0.0561 to 0.0824 m, with a mean of 0.0626 m; while the mean absolute error (MAE) ranged from 0.0396 to 0.0698 m, with a mean of 0.0516 m. These values indicate that the absolute deviations between simulated and observed water levels generally remained within an acceptable range. The Nash–Sutcliffe efficiency coefficient (NSE) ranged from 0.5972 to 0.7395, with a mean of 0.6960, suggesting that the model had adequate simulation capability for most monitoring stations during the dry season (Figure 4); for the Huangtugou Station with a relatively low NSE value, further investigation into parameters including upstream–downstream channel roughness and cross-section geometry is required to improve the overall model accuracy.

Table 2. Hydrodynamic simulation efficiency and error evaluation.

Station	RMSE	MAE	NSE
Xinghua	0.056	0.044	0.717
Fanchuan	0.056	0.040	0.711
Sanduo	0.061	0.051	0.681
Qintong	0.058	0.049	0.733
Taizhou	0.061	0.052	0.656
Huangtugou	0.082	0.069	0.597
Tangzi Town	0.062	0.055	0.709
Shenlun	0.060	0.050	0.719
Funing	0.066	0.053	0.739

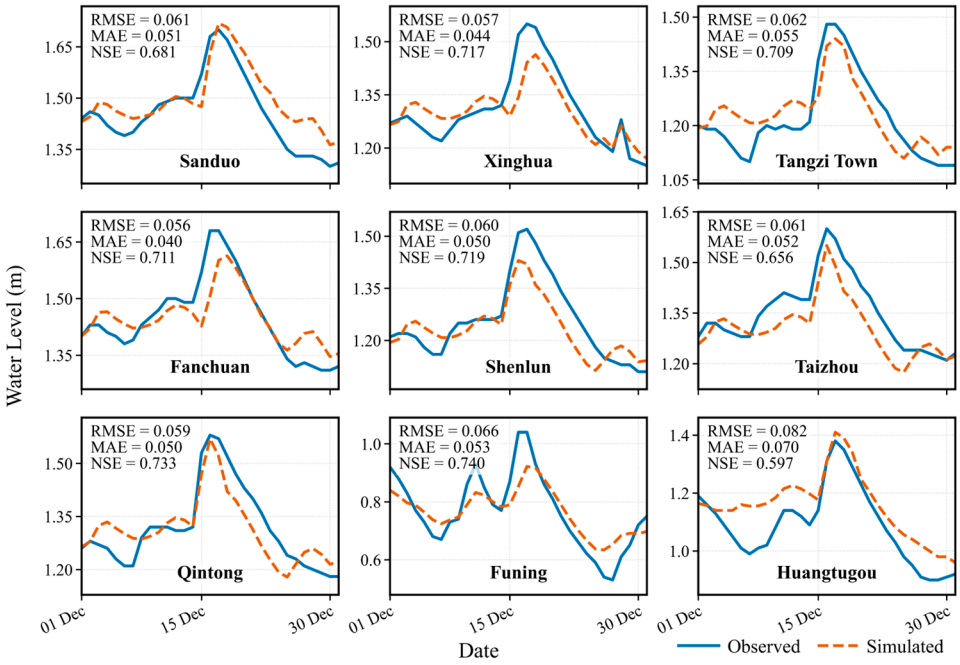


Figure 4. Parameter calibration process of the hydrodynamic model.

Calibration performance varied among the nine stations. The absolute error metrics and NSE describe different aspects of model performance. In particular, NSE is normalized by the variance of the observed series and is therefore sensitive to the magnitude of water level variability. Consequently, NSE values cannot be compared across stations without also considering RMSE, MAE, and the observed water level variation. For example, Funing had an RMSE of 0.066 m but the highest NSE of 0.739, whereas several stations with smaller RMSE values had lower NSE values. This difference indicates that a relatively high NSE does not necessarily correspond to the smallest absolute error.

Huangtugou showed the largest RMSE and MAE values, 0.082 and 0.069 m, respectively, together with the lowest NSE of 0.597. Therefore, its relatively weak performance cannot be attributed solely to the variance dependence of NSE. The discrepancy at this station may reflect the combined effects of local hydraulic structure operation, simplified representation of secondary channels and lateral exchanges, uncertainty in cross-sectional geometry and roughness, and differences between the prescribed and actual boundary conditions. Because the contributions of these factors were not separately quantified, they are interpreted as potential sources of uncertainty rather than confirmed causes. Model-derived results for Huangtugou should therefore be interpreted with greater caution than those for the better-performing stations.

The calibration results support comparative scenario analysis, but the influence of station-specific error and parameter uncertainty on the derived replenishment requirements remains a limitation.

3.2. Water Level Responses of the River Network Under Upstream Flow Gradients

Under upstream replenishment discharge gradients of 40–400 m^3/s, water levels at all nine control stations in the study area increased monotonically with increasing discharge. The mean station water level rose from 0.736 m under the 40 m^3/s scenario to 1.652 m under the 400 m^3/s scenario, an overall increase of 0.916 m. The response magnitude differed markedly among stations, indicating that upstream replenishment is not transmitted uniformly in space after entering the plain river network, but is jointly affected by river network connectivity, conveyance pathways, local cross-sectional conditions, and engineering control patterns.

In terms of station water level ranges (Table 3, Figure 5), Taizhou Station maintained relatively high water levels under all discharge scenarios. Its water level increased from 0.90 m to 1.90 m, an increase of 1.00 m, which was the largest water level rise in the simulations. Fanchuan and Qintong stations each increased by 0.98 m, Sanduo Station by 0.97 m, Shenlun Station by 0.96 m, and Xinghua and Tangzi Town stations each by 0.95 m, indicating clear responses to changes in replenishment discharge. In contrast, Huangtugou Station increased by 0.83 m and Funing Station by only 0.63 m, suggesting relatively weak water level responses to upstream replenishment at these stations. As discharge increased from 40 to 400 m^3/s, the inter-station water level difference expanded from 0.47 m to 0.84 m, indicating more pronounced spatial differentiation of regional water levels under high replenishment conditions.

Table 3. Simulated water levels at key stations under upstream flow gradient scenarios.

Discharge *	Xinghua	Fanchuan	Sanduo	Qintong	Taizhou	Huang-tugou	Tangzi Town	Shenlun	Funing
40	0.76	0.88	0.86	0.76	0.90	0.62	0.69	0.72	0.43
80	0.79	0.91	0.89	0.79	0.94	0.65	0.72	0.75	0.45
120	0.85	0.98	0.96	0.86	1.00	0.7	0.78	0.81	0.48
160	0.94	1.07	1.05	0.95	1.09	0.77	0.87	0.9	0.54
200	1.05	1.18	1.15	1.06	1.20	0.86	0.97	1.01	0.6
240	1.17	1.30	1.28	1.18	1.33	0.97	1.09	1.13	0.68
280	1.29	1.43	1.41	1.31	1.46	1.08	1.22	1.26	0.76
320	1.43	1.57	1.54	1.45	1.6	1.2	1.35	1.39	0.85
360	1.57	1.71	1.68	1.59	1.75	1.32	1.49	1.53	0.95
400	1.71	1.86	1.83	1.74	1.90	1.45	1.64	1.68	1.06

* Discharge is expressed in m^3/s; water level is measured in m.

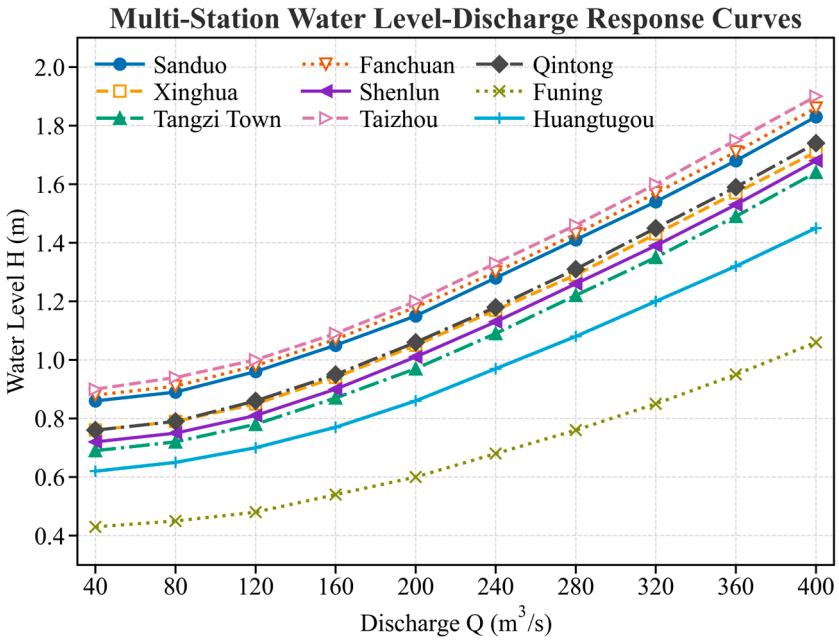


Figure 5. Stage–flow response curves at each station.

Within the 40–400 m^3/s scenario range and under fixed boundary and sluice pump rules, quadratic polynomials effectively represented the response relationships between station water levels and upstream replenishment discharge. The fitted R^2 values for all nine stations exceeded 0.998, with a mean of 0.998708, indicating that the quadratic function form could stably describe water level responses caused by changes in upstream replenishment discharge within the discharge range set in this study. The quadratic coefficients were positive for all stations, indicating that the marginal water level response to discharge increased with increasing replenishment discharge. When dH/dQ was used to characterize the marginal response, station responses were approximately 0.000597–0.001356 $m/(m^3/s)$ under the 40 m^3/s condition and increased to 0.002966–0.004408 $m/(m^3/s)$ under the 400 m^3/s condition. Taizhou Station showed the strongest marginal response in the high discharge range, whereas Funing Station exhibited the weakest response under both low and high discharge conditions (Table 4).

Table 4. Quadratic polynomial fitting coefficients for stage–flow response relationships.

Station	Quadratic Coefficient	Linear Coefficient	Constant Term	R^2 *
Xinghua	4.00×10^{-6}	0.000979	0.6941	0.998384
Fanchuan	4.05×10^{-6}	0.001032	0.8125	0.998734
Sanduo	3.98×10^{-6}	0.001033	0.7926	0.998592
Qintong	4.05×10^{-6}	0.001032	0.6925	0.998734
Taizhou	4.29×10^{-6}	0.000980	0.8375	0.998747
Huangtugou	3.76×10^{-6}	0.000723	0.5711	0.998607
Tangzi Town	4.17×10^{-6}	0.000888	0.6300	0.998769
Shenlun	4.07×10^{-6}	0.000966	0.6546	0.998453
Funing	3.29×10^{-6}	0.000334	0.4038	0.999357

* R^2 indicates the fitting performance of the regression equation. The high coefficients of determination reflect the smooth interpolation of ten deterministic scenario points generated with fixed boundaries and operation rules. They should not be interpreted as independent evidence of predictive accuracy. The fitted functions are valid only within the simulated range of 40–400 m^3/s and under the stated scenario assumptions.

The linear coefficient reflects the initial response sensitivity under low discharge increments. Sanduo Station had the highest linear coefficient, followed by Fanchuan and Qintong stations, indicating that these stations exhibited clear water level increases during the initial stage of replenishment. Funing Station had the lowest linear coefficient, indicating a weak direct response to upstream replenishment. In terms of the quadratic coefficient, Taizhou Station was the highest and Funing Station the lowest. Considering simulated water levels, response slopes, and fitted parameters, Taizhou, Fanchuan, Sanduo, and Qintong can be regarded as relatively sensitive stations in terms of replenishment response, whereas Huangtugou and Funing are weak response stations that require particular attention in subsequent water level compliance assessment.

3.3. Hydrologically Derived Candidate Water Level Benchmarks

Based on frequency analysis of winter water level series from 2006 to 2021, relatively complete winter water level samples were obtained for all nine control stations (Figure 6), with 1444 winter records at each station. Mean winter water levels differed markedly in space, with station means ranging from 0.765 to 1.202 m and a regional mean of 1.091 m. Among them, Fanchuan, Taizhou, and Sanduo stations had relatively high mean winter water levels of 1.202 m, 1.201 m, and 1.195 m, respectively; Funing and Huangtugou stations had markedly lower mean water levels of 0.765 m and 0.924 m, respectively. These results indicate that winter water levels in the study area do not share a unified regional benchmark, and that low water backgrounds and water level reference values need to be identified separately for each station.

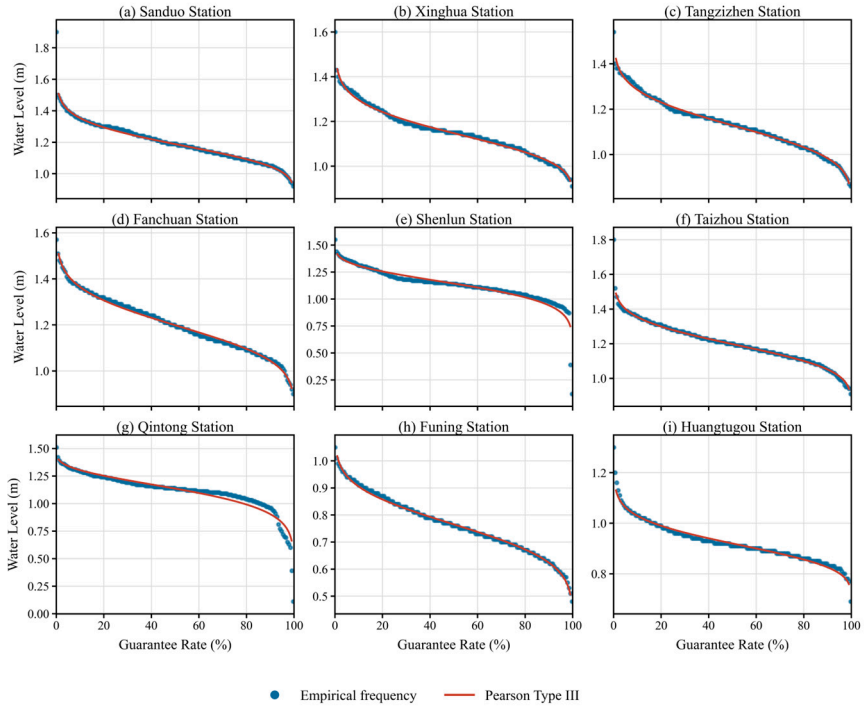


Figure 6. Frequency fitting of winter water levels at the stations.

Overall, the Pearson type III frequency curves were able to fit the winter water level distributions at each station, with fitted R^2 values of 0.8892–0.9957, RMSE values of 0.0072–0.0500 m, and MAE values of 0.0049–0.0307 m. Funing Station showed the best goodness of fit, whereas Shenlun Station showed relatively lower fit performance. This suggests that low water sequences at some stations are more strongly affected by local regulation or extreme low water processes, and that subsequent water level determination should be interpreted comprehensively using results from multiple methods. These

diagnostic results support the adequacy of P-III as a working distribution for the present water level records, but they should not be interpreted as demonstrating its superiority over probability distributions that were not evaluated in this study.

Spatially, Funing Station had the lowest water levels under all guarantee rate conditions. Its 90% and 75% guarantee rate water levels were 0.63 m and 0.69 m, respectively, which were substantially lower than those of other stations. The 90% and 75% guarantee rate water levels at Huangtugou Station were 0.84 m and 0.87 m, respectively, also indicating relatively low levels. In contrast, the water levels at Taizhou, Sanduo, Fanchuan, and Xinghua stations under the 90% guarantee rate were 1.05 m, 1.05 m, 1.05 m, and 1.01 m, respectively, showing relatively high winter water level guarantee conditions. These differences indicate that if a unified guarantee rate is used as the hydrological reference for water levels, the corresponding absolute water levels differ greatly among stations.

Overall, hydrological frequency methods provide historical hydrological references for identifying winter water level targets in the study area (Figure 7). These values can serve as important candidates for subsequent comparison of water level targets. Because frequency methods mainly characterize the occurrence probability of historical water levels, the results in this section should not be directly equated with final water level targets. The frequency-derived water level results should be combined with station-specific water level conditions to further determine integrated water level targets for inversion of upstream replenishment discharge thresholds.

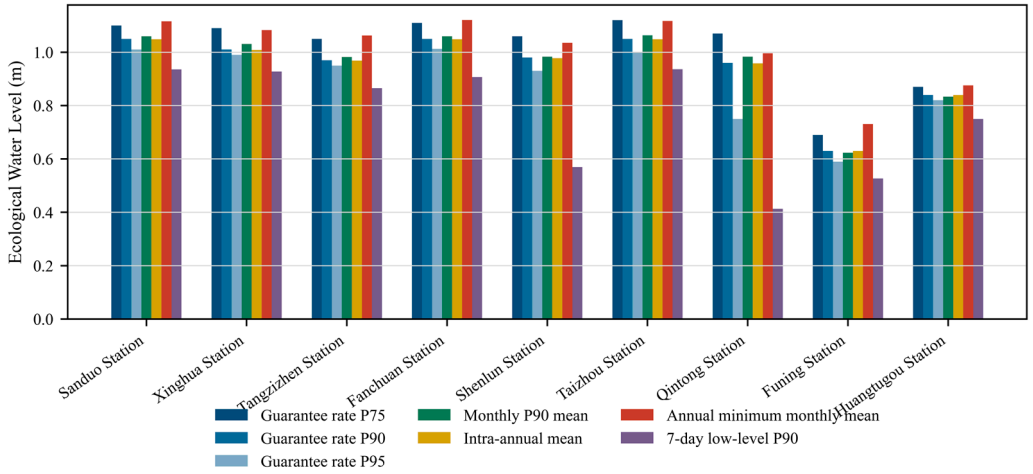


Figure 7. Comparison of water levels corresponding to different water level determination methods at each station.

3.4. Scenario-Specific Replenishment Requirements

The winter water levels of the nine stations ranged from 0.413 to 1.121 m. After conversion based on the fitted Q-H relationships at each station (Figure 8), the replenishment discharge required to meet water level targets at the station scale ranged from 153.94 to 268.49 m^3/s (Table 5), corresponding to fitted guarantee rates of 12.06–60.70% (Figure 9).

The most difficult water level target to satisfy was the annual minimum monthly mean target at Funing Station. The corresponding water level was 0.731 m, requiring a discharge of 268.49 m^3/s, with a discharge guarantee rate of 12.06%. Under the condition that water levels at other stations are already satisfied, this station–method combination forms the final controlling constraint for the overall replenishment discharge of the study area.

Cross-station comparison among stations shows that Funing Station had the highest bound discharge requirement (268.49 m^3/s, controlled by the annual minimum monthly mean method), whereas Tangzi Town Station controlled the regional minimum replenishment threshold (153.94 m^3/s).

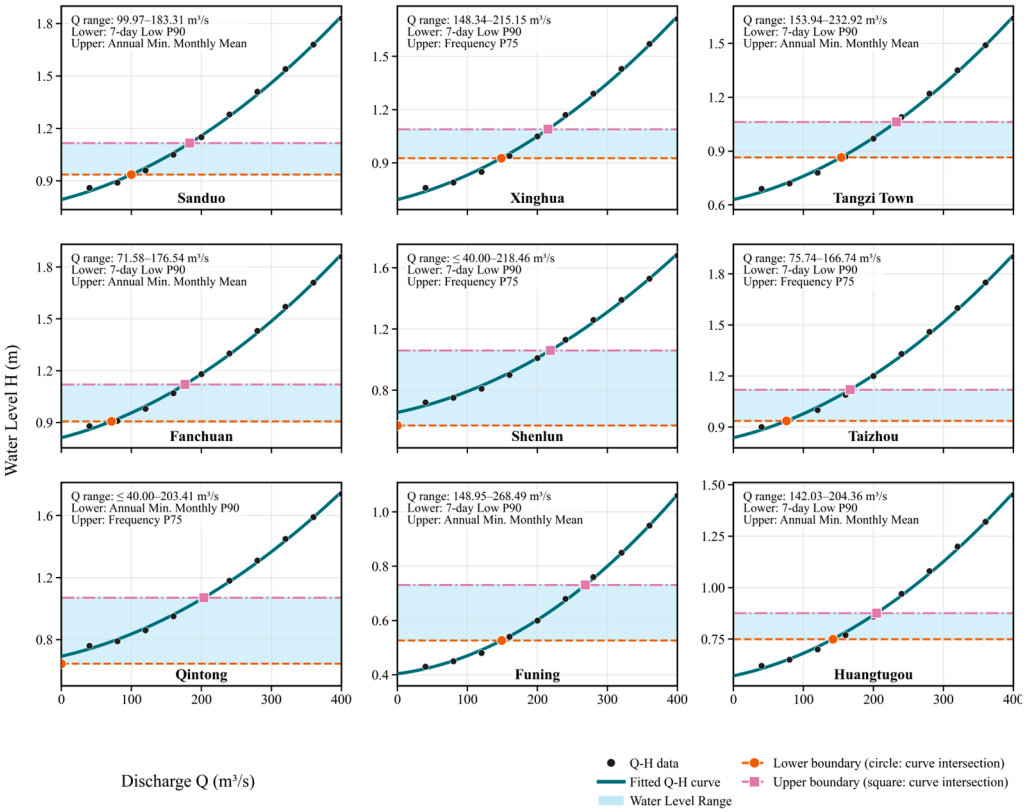


Figure 8. Relationship between station water levels and corresponding discharge.

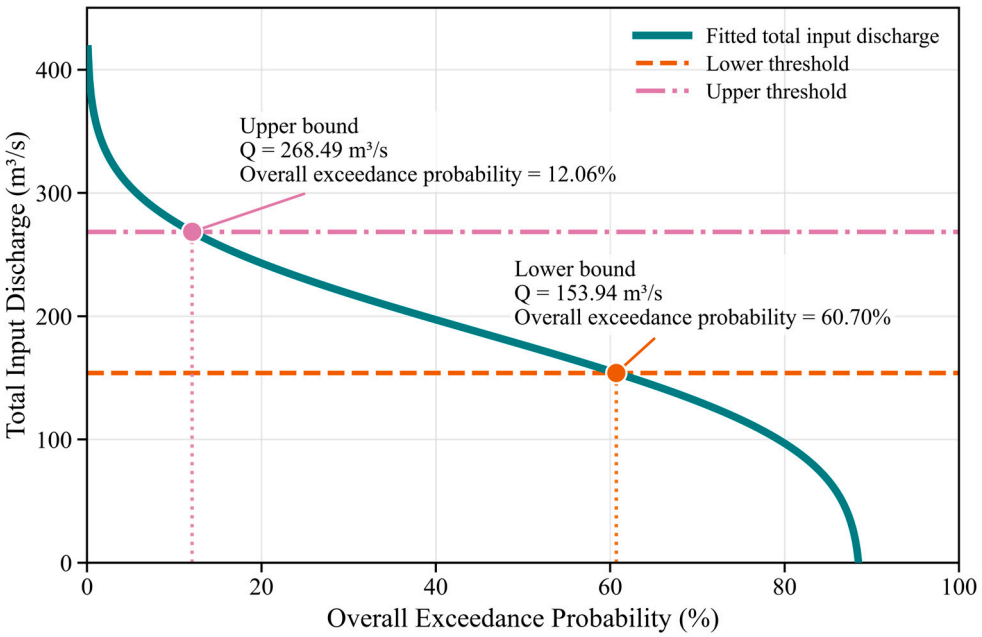


Figure 9. Regional total input discharge guarantee.

Comparison among methods indicates that the 7-day low water frequency P90 method had the lowest regional controlling discharge (153.94 m^3/s, with a guarantee rate of 60.70%) and therefore the best attainability under a water saving objective. The annual minimum monthly mean method had the highest controlling discharge (268.49 m^3/s, with a guarantee rate of 12.06%), representing the most water-demanding benchmark among the methods evaluated.

Table 5. Minimum discharge and guarantee rate corresponding to the hydrological water level targets at each station.

Station	Required Replenishment Discharge [2] (m^3/s)	Guarantee Rate Fitted Percent (%)	Controlling Method
Xinghua	148.34	63.14	7-day Low P90
Fanchuan	71.58	84.42	7-day Low P90
Sanduo	99.97	79.30	7-day Low P90
Qintong	≤40.00 [1]	87.25	Annual Min. Monthly P90
Taizhou	75.74	83.85	7-day Low P90
Huangtugou	142.03	66.57	7-day Low P90
Tangzi Town	153.94	60.70	7-day Low P90
Shenlun	≤40.00	87.25	7-day Low P90
Funing	148.95	62.88	7-day Low P90

[1] Table note: ≤40.00 m^3/s indicates that the water level target is lower than or equal to the lowest simulated scenario; it does not mean that replenishment is entirely unnecessary under observed conditions. [2] Table note: Required Replenishment Discharge indicates the discharge required to meet the water level target derived from hydrological methods.

4. Discussion

4.1. Complementing Conventional Hydrological Statistical Methods

Conventional hydrological statistical methods are based on historical water level or discharge series and can characterize the frequency properties and guarantee levels of dry season hydrological processes, making them important references for determining ecological water levels. In plain river network areas with relatively complete data, guarantee rate water levels, duration curves, and frequency analysis results have the advantages of clear calculation procedures, reproducible results, and ease of interpretation by management agencies. However, hydrological frequency methods mainly reflect the statistical distribution of historical hydrological processes and cannot directly determine whether a given water level can maintain suitable water depth, flow velocity, and aquatic habitat requirements [30,31]. Therefore, in the Lixiahe region, where artificial regulation is strong and hydrodynamic processes are relatively weak, determining ecological water levels solely on the basis of historical low water levels or a particular guarantee rate water level may overlook the integrated responses of biological communities to water depth, velocity, water quality, and connectivity.

From a methodological perspective, hydrological frequency methods provide the long-term series context, whereas hydrodynamic models provide water level response relationships under engineering operation boundaries. Combining the two can avoid the limitations of a single method: hydrological statistical results prevent the analysis from depending entirely on a limited set of simulation results, while hydrodynamic responses prevent ecological water levels from being reduced to historical statistical quantiles. This coupling enables ecological water level targets to be converted into operational upstream replenishment discharge thresholds. Such an approach is particularly suitable for plain river network regions, because water level processes in these areas are jointly influenced by natural inflow, external replenishment, sluice pump operation, and network connectivity, and ecological water level maintenance requires both hydrological justification and engineering feasibility.

This study used multiple hydrological statistical methods to generate water level target candidates and converted water level targets into replenishment thresholds through hydrodynamic responses. The coupling performed here addresses operational attainability, not ecological sufficiency. It prevents a hydrological benchmark from being used without checking whether it can be achieved through the regulated network, but it does not establish

that attaining the benchmark protects local biota. Verification based on ecological responses still requires further research.

4.2. Mechanisms Controlling Stage–Flow Responses in Plain River Networks

As a typical plain river network, the Lixiahe region does not exhibit a simple relationship between upstream discharge and downstream water level as found in a single channel. The stage–upstream replenishment discharge response relationships constructed in this study show that the same increment in external replenishment may produce different magnitudes of water level rise at different stations. This spatial difference reflects the complexity of replenishment transmission in plain river networks. After upstream input discharge enters the network, it is affected by multiple factors, including network topology [21,22], branching and confluence, lake storage regulation, and downstream boundary control.

River network connectivity determines whether replenishment discharge can be effectively transmitted to ecologically sensitive reaches. Compared with a single channel, flow pathways in plain river networks are characterized by multiple channels, numerous nodes, and weak directionality. Although some areas may receive total replenishment input, actual hydrodynamic improvement may be limited because of gate control, local barriers, or insufficient hydraulic gradient. In addition, lakes and wide shallow reaches have obvious storage regulation effects, which may weaken the immediate response of local water levels to upstream replenishment, causing water level changes to appear as gradual rises or reduced marginal responses. Furthermore, sluice pump operating modes alter internal water level boundaries and flow direction structures within the river network, so the same total replenishment amount can generate different spatial water level distributions under different operating states.

Therefore, the amount of replenishment in a plain river network cannot be directly equated with the effective ecological replenishment amount. The effect of replenishment depends not only on the magnitude of input discharge from upstream hubs such as Jiangdu and Gaogang but also on whether replenishment pathways cover ecologically sensitive reaches, whether key nodes have sufficient conveyance capacity, and whether post-replenishment water levels and velocities simultaneously meet ecological requirements. The significance of the stage–flow response curves lies in converting this complex hydrodynamic transmission process into comparable station response functions, thereby providing a quantitative basis for identifying replenishment-sensitive stations, weak response reaches, and key control nodes.

4.3. Implications for Dry Season Water Replenishment Operations

The core objective of dry season water replenishment is not simply to raise water levels across the entire region, but to improve replenishment efficiency and reduce engineering operating costs while satisfying ecological bottom-line requirements. By identifying upstream replenishment discharge thresholds based on water level targets and stage–flow response relationships, this study provides references for winter operation at three levels: determining the minimum replenishment requirements of key water level stations; comparing the response sensitivity of different stations to upstream replenishment and identifying areas with higher or lower replenishment efficiency; and converting water-level targets into executable discharge control indicators for hubs such as Jiangdu and Gaogang. Compared with replenishment schemes based solely on empirical operation or historical mean discharge, this method more clearly indicates how much water should be supplied and which areas may remain insufficiently supported.

From the perspective of engineering management, dry season replenishment can adopt a graded operation strategy. First, the minimum water level should be used as a bottom-line

constraint to ensure that key stations and key reaches do not fall below ecological control water levels. Second, after the bottom-line target is met, sluice pump joint operation [18] can be further optimized in combination with flow velocity, water quality, and river network connectivity requirements to improve hydrodynamic conditions in weak exchange reaches. Finally, under continuous dry conditions or insufficient external inflow, priority should be given to ecologically sensitive areas and weak response areas, and local engineering control measures should be combined to improve replenishment effectiveness. This approach helps shift replenishment from simple discharge supply toward integrated management of water level targets, replenishment pathways, sluice pump regulation, and ecological responses.

At the same time, replenishment thresholds should not be understood as fixed single operating values, but rather as management references under specific winter boundary conditions, model scenarios, and ecological target constraints. In actual operation, upstream water availability, downstream drainage conditions, regional flood control safety, water quality improvement needs, and coordination among different water use sectors must also be considered. For some reaches with weak responses to replenishment, simply increasing total replenishment discharge may not substantially improve ecological water levels or flow velocity conditions and may instead introduce local high water level risks. Water level attainment does not imply water quality attainment. The effect of replenishment depends on the quality of source water, background conditions in receiving reaches, residence time, and the operation of drainage outlets. Operational application should therefore include source and receiving water monitoring and predefined water quality constraints or suspension conditions. Therefore, subsequent engineering applications can build on the threshold identification in this study to further investigate joint sluice pump operation, multi-inlet replenishment combinations, and coupled hydrodynamic water quality optimization [32,33].

4.4. Method Uncertainty, Data Limitations, and Applicability

The proposed method still has certain uncertainties. First, hydrodynamic model results are affected by river network generalization, cross-section data accuracy, roughness parameters, boundary conditions, and sluice pump operating rules. Plain river networks contain many sluices and pumps with complex operating states. If fixed openings, typical operating conditions, or simplified boundaries are adopted for some engineering nodes in the model, the simulation results are more suitable for scenario comparison and response trend identification than for direct interpretation as precise forecasts under arbitrary operating conditions. Although spatial variability in Manning roughness was represented using reach-specific coefficients, its possible temporal variation within and between winters was not explicitly modeled because corresponding time-resolved observations of vegetation, sediment, and channel maintenance conditions were unavailable. Consequently, the simulated water levels and derived replenishment thresholds remain conditional on the calibrated winter roughness configuration. Second, the stage–flow response curves were fitted under specified replenishment gradients and boundary conditions, and their applicability is limited to the discharge range covered by the model scenarios. If operating discharge exceeds this range, or if the replenishment proportion between Jiangdu and Gaogang changes substantially, scenario simulations should be repeated, or the response relationships should be revised. The estimated guarantee levels should be interpreted as hydrological benchmarks conditional on the 2006–2021 regulated period, rather than as permanent or biologically validated ecological thresholds. Their principal role is to support comparative screening and operational scenario assessment.

5. Conclusions

5.1. Main Findings

1. Under the specified winter boundaries and structure operation rules, the lowest regional controlling replenishment requirement among the evaluated hydrological benchmarks was 153.94 m^3/s. This value was controlled by Tangzi Town Station under the 7-day low water P90 benchmark. It should be interpreted as a scenario-specific water allocation reference, not as a biologically validated minimum ecological discharge.
2. Under the simulated conditions, when the replenishment discharge is 218.46–232.92 m^3/s, the strictest method water level requirements can be satisfied at 7–8 of the 9 stations, with the corresponding fitted guarantee rate decreasing from 30.00% to 23.87%. If water level targets are required to be satisfied at all stations, the discharge must be increased to 268.49 m^3/s, corresponding to a guarantee rate of 12.06%.
3. Among the different hydrological water level methods, the 7-day low water frequency P90 method has the lowest regional controlling discharge (153.94 m^3/s) and the highest guarantee rate at the control point (60.70%), making it more applicable from the perspective of water saving and attainability.
4. The annual minimum monthly mean benchmark produced the largest regional requirement (268.49 m^3/s) among the methods evaluated. This result indicates the highest water demand in the comparison; it does not by itself demonstrate a higher level of ecological protection.

5.2. Upstream Replenishment Flow Thresholds and Management Recommendations

Based on different water level methods and station Q-H response relationships, winter replenishment in the Lixiahe region can adopt graded threshold management. If water saving and attainability are prioritized, 153.94 m^3/s can be used as the reference threshold for the regional minimum replenishment discharge. This threshold is controlled by Tangzi Town Station under the 7-day low water frequency P90 method and corresponds to a fitted guarantee rate of 60.70%. When the operation target is raised to strict water level protection at most stations, the replenishment discharge needs to increase to 218.46–232.92 m^3/s, satisfying the strictest method targets at 7–8 of the 9 stations. If all control stations are required to reach the strictest water level targets, the discharge must reach 268.49 m^3/s. This threshold is controlled by Funing Station under the annual minimum monthly mean method and corresponds to a guarantee rate of only 12.06%; in practical application, it should be evaluated comprehensively in relation to water source conditions, flood control safety, and local high water level risks.

Therefore, in engineering operation, the replenishment threshold should not be interpreted as a fixed single value. Instead, it should be dynamically selected among lower bound protection, enhanced multi-station protection, and strict whole-region protection according to water availability, ecological protection level, and the demands of key reaches. For weak response stations such as Funing and Huangtugou, simply increasing total replenishment discharge may have limited efficiency; future operation should improve replenishment effectiveness by combining joint sluice pump regulation with optimization of local replenishment pathways.

5.3. Future Research

Future research can proceed in three directions. First, aquatic biological, water quality, and habitat monitoring data should be supplemented through field ecological sampling and assessment [34,35], so that hydrological statistical ecological water levels can be cross-validated against biological response thresholds [36,37] and the ecological interpretability of water level targets can be improved [38]. Second, scenarios involving joint sluice pump

operation, multi-inlet replenishment proportions, and downstream boundary variations should be further refined to evaluate replenishment efficiency, local high water level risks, and improvements in weak exchange reaches under different engineering combinations. Third, model validation over longer periods and independent years should be conducted, and uncertainty analysis should be performed for Pearson type III frequency fitting, Q-H curve inversion, and missing data treatment, so as to provide confidence intervals and risk boundaries for engineering application of ecological replenishment thresholds.

Author Contributions: Conceptualization, Y.Z. and G.N.; methodology, Y.Z., G.S., and Y.X.; formal analysis, T.D.; investigation, Y.Z., and T.C.; data curation, Y.Z. and Y.X.; writing—original draft preparation, Y.Z.; writing—review and editing, Y.Z. and G.N.; visualization, G.N.; supervision, G.N. All authors have read and agreed to the published version of the manuscript.

Funding: This research was funded by the National Key R&D Program Young Scientist Project (2024YFC3214100); Young Scientists Fund (C Class) of the National Natural Science Foundation of China (No. 52409050); National Natural Science Foundation of China (Joint Fund for Research on Yellow River Water) (U2243601-02); Hebei Provincial Water Conservancy Science and Technology Program Project (2025-70); Basic Scientific Research Fund of IWHR (90022605).

Institutional Review Board Statement: Not applicable.

Informed Consent Statement: Not applicable.

Data Availability Statement: The original data presented in this study are openly available in Zenodo at https://zenodo.org/records/21270197 (accessed on 9 July 2026). The datasets include MIKE model setup files, river network data, water level data, and discharge data. The original hydrological and river network datasets were obtained from the public data portals. Users should comply with the terms and conditions of the original data providers where applicable.

Acknowledgments: The authors thank the providers of the historical water level data, discharge data, and river cross-section data used in this study. During the preparation of this manuscript, the authors used Codex (version 26.707.62119) for assistance with preliminary data analysis and language polishing. The authors have reviewed and edited the output and take full responsibility for the content of this publication.

Conflicts of Interest: The authors declare no conflicts of interest.

References

1. Tang, H.; Yuan, S.; Cao, H. Theory and practice of hydrodynamic reconstruction in plain river networks. *Engineering* **2023**, *24*, 202–211. [CrossRef]
2. Gao, H.; Wang, Q.; Zhou, Z.; Wu, W.; Wang, W.; Li, Y.; Hu, J.; Li, P.; Zhang, Y.; Hu, W. Optimizing hydrodynamic regulation in coastal plain river networks in eastern China: A MIKE11-based partitioned water allocation framework for flood control and water quality enhancement. *Water* **2025**, *17*, 1829. [CrossRef]
3. Zhu, Q.; Fang, K.; Zhu, D.; Li, X.; Chen, X.; Han, S.; Chen, F.; Gao, C.; Sun, J.; Tang, R.; et al. Simulation and analysis of water quality improvement measures for plain river networks based on Infoworks ICM model: Case study of Baoying County, China. *Water* **2024**, *16*, 2698. [CrossRef]
4. Poff, N.L.; Allan, J.D.; Bain, M.B.; Karr, J.R.; Prestegaard, K.L.; Richter, B.D.; Sparks, R.E.; Stromberg, J.C. The natural flow regime. *BioScience* **1997**, *47*, 769–784. [CrossRef]
5. Tharme, R.E. A global perspective on environmental flow assessment: Emerging trends in the development and application of environmental flow methodologies for rivers. *River Res. Appl.* **2003**, *19*, 397–441. [CrossRef]
6. Tickner, D.; Opperman, J.J.; Abell, R.; Acreman, M.; Arthington, A.H.; Bunn, S.E.; Cooke, S.J.; Dalton, J.; Darwall, W.; Edwards, G.; et al. Bending the curve of global freshwater biodiversity loss: An emergency recovery plan. *BioScience* **2020**, *70*, 330–342. [CrossRef] [PubMed]
7. Gleeson, T.; Wang-Erlandsson, L.; Zipper, S.C.; Porkka, M.; Jaramillo, F.; Gerten, D.; Fetzer, I.; Cornell, S.E.; Piemontese, L.; Gordon, L.J.; et al. The water planetary boundary: Interrogation and revision. *One Earth* **2020**, *2*, 223–234. [CrossRef]
8. Albert, J.S.; Destouni, G.; Duke-Sylvester, S.M.; Magurran, A.E.; Oberdorff, T.; Reis, R.E.; Winemiller, K.O.; Ripple, W.J. Scientists' warning to humanity on the freshwater biodiversity crisis. *Ambio* **2021**, *50*, 85–94. [CrossRef] [PubMed]

9. van Rees, C.B.; Waylen, K.A.; Schmidt-Kloiber, A.; Thackeray, S.J.; Kalinkat, G.; Martens, K.; Domisch, S.; Lillebo, A.I.; Hermoso, V.; Grossart, H.P.; et al. Safeguarding freshwater life beyond 2020: Recommendations for the new global biodiversity framework from the European experience. *Conserv. Lett.* **2021**, *14*, e12771. [CrossRef]
10. Maasri, A.; Jahnig, S.C.; Adamescu, M.C.; Adrian, R.; Baigun, C.; Baird, D.J.; Batista-Morales, A.; Bonada, N.; Brown, L.E.; Cai, Q.; et al. A global agenda for advancing freshwater biodiversity research. *Ecol. Lett.* **2022**, *25*, 255–263. [CrossRef] [PubMed]
11. Dudgeon, D. Multiple threats imperil freshwater biodiversity in the Anthropocene. *Curr. Biol.* **2019**, *29*, R960–R967. [CrossRef] [PubMed]
12. Zhang, C.; Wang, L.; Zhu, H.; Tang, H. Integrated hydrodynamic model for simulation of river-lake-sluice interactions. *Appl. Math. Model.* **2020**, *83*, 90–106. [CrossRef]
13. Huang, S.; Xia, J.; Wang, Y.; Wang, W.; Zeng, S.; She, D.; Wang, G. Coupling machine learning into hydrodynamic models to improve river modeling with complex boundary conditions. *Water Resour. Res.* **2022**, *58*, e2022WR032183. [CrossRef]
14. Zhou, H.; Liu, J.; Gao, C.; Li, W.; Ou, S.; Zhou, Y.; Luan, Q. Copula-based joint impact assessment of rainfall and tidal level on flood risk in tidal-influenced plain river network areas, Taihu Lake Basin. *J. Hydrol.* **2025**, *653*, 132785. [CrossRef]
15. Lu, M.; Li, M.; Shi, H.; Bai, Y.; Xu, Y.; Lin, Z. Combined effects of rainfall, structural complexity and human regulation on process connectivity in a plain river network. *J. Hydrol. Reg. Stud.* **2026**, *65*, 103353. [CrossRef]
16. Jiang, C.; Luo, L.; Zhou, J.; Fu, G.; Chen, X. Spatio-temporal variation of water quality in Lixia River Watershed associated with the operation of a water diversion project. *Water Resour.* **2024**, *51*, 72–83. [CrossRef]
17. Liu, J.; Ding, R.; Chen, Y.; Zhu, W.; Fan, Z.; Ma, J. Assessment and optimization of water resources regulation for river networks in the tidal plain: A case study of the Qingsong area in Shanghai. *Water* **2022**, *14*, 3523. [CrossRef]
18. Al-Jawad, J.Y.; Alsaffar, H.M.; Bertram, D.; Kalin, R.M. Optimum socio-environmental flows approach for reservoir operation strategy using many-objectives evolutionary optimization algorithm. *Sci. Total Environ.* **2019**, *651*, 1877–1891. [CrossRef] [PubMed]
19. Lv, S.; Li, C.; Gao, F. Hydrodynamic features and water ecology improvement of Yuehai Lake based on ecological water diversion. *Alex. Eng. J.* **2022**, *61*, 2909–2918. [CrossRef]
20. Meng, Z.; Tao, Y.; Guan, X.; Zhou, C.; Gu, L.; Liu, X. Research on sluice-pump operation for enhancing hydrodynamic conditions and water quality improvement mechanisms in polder areas. *J. Hydroinform.* **2025**, *27*, 1801–1818. [CrossRef]
21. Chen, X.; Chen, L.; Stone, M.C.; Acharya, K. Assessing connectivity between the river channel and floodplains during high flows using hydrodynamic modeling and particle tracking analysis. *J. Hydrol.* **2020**, *583*, 124609. [CrossRef]
22. Xiao, Y.; Liu, J.; Gualtieri, C.; Fu, J.; Gu, R.; Wang, Z.; Zhang, T.; Zhou, J. The effect of natural and engineered hydraulic conditions on river-floodplain connectivity using hydrodynamic modeling and particle tracking analysis. *J. Hydrol.* **2022**, *615*, 128578. [CrossRef]
23. Wang, Y.; Lei, C.; Ye, S.; Wang, Q.; Xu, Y.; Zhang, J.; Xu, Y. Assessing the impact of river changes on flood regulation capacity using a coupled flood model in an urbanized plain river network region. *J. Hydrol. Reg. Stud.* **2024**, *55*, 101925. [CrossRef]
24. Zhu, Y.; Chen, Q.; Zhang, Y.; Li, Q.; Chen, J.; Song, Y.; Yang, X. Simulation Analysis of Water Quality Improvement Effect of the Yangtze River Diversion on the Frontier of the Eastern Route of the South-to-North Water Transfer Project. *J. China Hydrol.* **2021**, *41*, 25–31. (In Chinese with English Abstract) Available online: https://link.cnki.net/doi/10.19797/j.cnki.1000-0852.20200466 (accessed on 18 August 2026).
25. McHugh, A.R.; Suro, T.P.; Sullivan, S.L.; Williams, B.M. *Streamflow Characteristics and Trends in New Jersey, Water Years 1903–2017*; U.S. Geological Survey: Reston, VA, USA, 2024; 59p. [CrossRef]
26. Xie, Y.; Guo, S.; Zhong, S.; Wang, X.; Tian, J.; Liang, Z. A novel time-varying P-III distribution curve fitting model to estimate design floods in Three Gorges Reservoir operation period. *Hydrology* **2024**, *11*, 203. [CrossRef]
27. Zhang, T.; Dong, Z.; Li, Y.; Shen, Q.; Huang, Y.; Chen, C.; Zhou, Q.; Zhang, Y. Optimum ecological water level of water-carrying lake based on the relationship between water quality and water level. *J. Lake Sci.* **2022**, *34*, 1670–1682. [CrossRef]
28. Wang, H.; Zheng, Y.; Zhang, H.; Gao, W. Ecological water level and its safeguard measures in Lake Dongting. *J. Lake Sci.* **2020**, *32*, 1529–1538. [CrossRef]
29. Zhang, C.; Chen, W.; Huang, F. Determining the suitable ecological water level based on the response relationship between landscape connectivity and water level: A case study of Poyang Lake, China. *Ecol. Indic.* **2025**, *175*, 113562. [CrossRef]
30. Fox, J.T.; Magoulick, D.D. Hydrologic and environmental thresholds in stream fish assemblage structure across flow regimes. *Ecol. Indic.* **2022**, *144*, 109500. [CrossRef]
31. Praskievicz, S.; Luo, C. Assessment of flow-ecology relationships for environmental flow standards: A synthesis focused on the southeast USA. *Hydrol. Sci. J.* **2020**, *65*, 571–582. [CrossRef]
32. Jiang, Q.; Li, J.; Sun, Y.; Huang, J.; Zou, R.; Ma, W.; Guo, H.; Wang, Z.; Liu, Y. Deep-reinforcement-learning-based water diversion strategy. *Environ. Sci. Ecotechnol.* **2024**, *17*, 100298. [CrossRef] [PubMed]
33. Luo, W.; Wang, C.; Zhang, Y.; Zhao, J.; Huang, Z.; Wang, J.; Zhang, C. A deep reinforcement learning approach for joint scheduling of cascade reservoir system. *J. Hydrol.* **2025**, *651*, 132515. [CrossRef]

34. Perry, W.B.; Seymour, M.; Orsini, L.; Jams, I.B.; Milner, N.; Edwards, F.; Harvey, R.; de Bruyn, M.; Bista, I.; Walsh, K.; et al. An integrated spatio-temporal view of riverine biodiversity using environmental DNA metabarcoding. *Nat. Commun.* **2024**, *15*, 4372. [CrossRef] [PubMed]
35. Carraro, L.; Machler, E.; Wuthrich, R.; Altermatt, F. Environmental DNA allows upscaling spatial patterns of biodiversity in freshwater ecosystems. *Nat. Commun.* **2020**, *11*, 3585. [CrossRef] [PubMed]
36. Birk, S.; Chapman, D.; Carvalho, L.; Spears, B.M.; Andersen, H.E.; Argillier, C.; Auer, S.; Baattrup-Pedersen, A.; Banin, L.; Beklioglu, M.; et al. Impacts of multiple stressors on freshwater biota across spatial scales and ecosystems. *Nat. Ecol. Evol.* **2020**, *4*, 1060–1068. [CrossRef] [PubMed]
37. Kuehne, L.M.; Dickens, C.; Tickner, D.; Messager, M.L.; Olden, J.D.; O'Brien, G.; Lehner, B.; Eriyagama, N. The future of global river health monitoring. *PLoS Water* **2023**, *2*, e0000101. [CrossRef]
38. Kaijser, W.; Musiol, M.; Schneider, A.R.; Prati, S.; Brauer, V.S.; Bayer, R.; Birk, S.; Brauns, M.; Dunne, L.; Enss, J.; et al. Meta-analysis-derived estimates of stressor-response associations for riverine organism groups. *Nat. Ecol. Evol.* **2025**, *9*, 2304–2321. [CrossRef] [PubMed]

Disclaimer/Publisher's Note: The statements, opinions and data contained in all publications are solely those of the individual author(s) and contributor(s) and not of MDPI and/or the editor(s). MDPI and/or the editor(s) disclaim responsibility for any injury to people or property resulting from any ideas, methods, instructions or products referred to in the content.